

Numerical Analysis on Added Resistance of Hydroelastic Body in Waves

Dong-Min Park*, Jung-Hyun Kim, Yonghwan Kim

Department of Naval Architecture and Ocean Engineering, Seoul National University, Seoul, Korea

*E-mail: foster@snu.ac.kr

HIGHLIGHT

- Added resistance of flexible floating body was obtained by using a coupled hydrodynamic-structural solver based on Rankine panel method and FEM modeling.
- A pressure integration method including an extension of the rigid body formula in the flexible body was suggested as well as a momentum conservation method.
- Added resistance of flexible body increased near the natural frequency of vertical mode and decreased near the similar wave length with the ship length.

1 INTRODUCTION

As ships increase in size, their relative stiffness decreases. For larger ship, the flexible body deformation becomes more important; as a result, many studies have been conducted to investigate the effects of flexibility on structural problems, such as maximum stress and fatigue damage amongst others. However, there have been very few studies investigating the effects of flexibility on added resistance.

In the present study, a fully coupled fluid-structure interaction model was used to compute the added resistance on a flexible body. In the computation of added resistance, two approaches were employed: a pressure integration method and a momentum conservation method. The pressure integration method included an extension of the rigid body formula in the flexible body formula. The momentum conservation method used the same formula for the rigid body and the flexible body. To the knowledge of the authors, it was not easy to find validation data for the added resistance on a flexible body. Therefore, an indirect validation was conducted by comparison of numerical results using different approaches: the pressure integration method and the momentum conservation method.

2 COMPUTATIONAL METHODS

The fluid domain was solved using a B-spline 3-D Rankine panel method, and the structural domain was modeled using a shell-element-based 3-D finite element model. The fluid model was coupled with the 3-D FE model via eigenvectors. The details are in the paper of Kim et al. (2012, 2015). As the name suggests, the added resistance can be obtained from the momentum at a faraway position. Regardless of if the body is a rigid or flexible body, the momentum conservation method has same formula. The mean horizontal forces are expressed as follows:

- Momentum conservation method

$$\begin{aligned}
 \vec{F}^{(2)} &= -\rho \iint_{S_f} \left[\frac{p}{\rho} \vec{n} + \vec{V}(\vec{V} \cdot \vec{n} - \vec{U} \cdot \vec{n}) \right] ds - \rho \int_{S_H} \int_{z=0}^{z=\zeta} \left[\frac{p}{\rho} \vec{n} + \vec{V}(\vec{V} \cdot \vec{n} - \vec{U} \cdot \vec{n}) \right] dz dl \\
 &= -\frac{\rho}{2} \iint_{S_f} (\nabla \phi \cdot \nabla \phi) \vec{n} ds - \rho \iint_{S_f} \nabla \phi (\nabla \phi \cdot \vec{n}) ds \\
 &\quad - \frac{\rho g}{2} \int_{S_H} \zeta^2 \vec{n} dl - \rho \int_{S_H} \zeta (\nabla \Phi \cdot \vec{n} - \vec{U} \cdot \vec{n}) \nabla \phi dl - \rho \int_{S_H} \zeta (\nabla \phi \cdot \vec{n}) \nabla \Phi dl
 \end{aligned} \tag{1}$$

From the formulation of added resistance on the rigid body, the added resistance of the flexible body could be extended. It is assumed that the order of lower flexible modes is the same order as that of the rigid body mode. The added resistance of the flexible body can be expressed as:

▪ Pressure integration method

$$\begin{aligned}
 \vec{F}^{(2)} = & \frac{1}{2} \rho g \int_{WL} [\zeta_I + \zeta_d - (\xi_{Tot,1,z})]^2 \frac{\vec{N}}{\sin \alpha} dl \\
 & - \rho \int_{WL} \left[\frac{\partial \Phi}{\partial t} - \vec{U} \cdot \nabla \Phi + \frac{1}{2} \nabla \Phi \cdot \nabla \Phi \right] [\zeta_I + \zeta_d - (\xi_{Tot,1,z})] \frac{(\vec{\xi}_{Rf} \times \vec{N})}{\sin \alpha} dl \\
 & - \rho \iint_{\bar{s}_B} \left[\frac{1}{2} \nabla(\phi_I + \phi_d) \cdot \nabla(\phi_I + \phi_d) \right] \vec{N} dS \\
 & - \rho \iint_{\bar{s}_B} \left[(\vec{\xi}_{Tot,1}) \cdot \nabla \left(\frac{\partial(\phi_I + \phi_d)}{\partial t} - (\vec{U} - \nabla \Phi) \cdot \nabla(\phi_I + \phi_d) \right) \right] \vec{N} dS \\
 & - \rho \iint_{\bar{s}_B} \left[(\xi_{Tot,2}) \cdot \nabla \left(\frac{\partial \Phi}{\partial t} - \vec{U} \cdot \nabla \Phi + \frac{1}{2} \nabla \Phi \cdot \nabla \Phi + gZ \right) \right] \vec{N} dS \\
 & - \rho \iint_{\bar{s}_B} \left[\frac{\partial(\phi_I + \phi_d)}{\partial t} - (\vec{U} - \nabla \Phi) \cdot \nabla(\phi_I + \phi_d) + g(\xi_{Tot,1,z}) \right] (\vec{\xi}_{Rf} \times \vec{N}) dS \\
 & - \rho \iint_{\bar{s}_B} \left[(\vec{\xi}_{Tot,1}) \cdot \nabla \left(\frac{\partial \Phi}{\partial t} - \vec{U} \cdot \nabla \Phi + \frac{1}{2} \nabla \Phi \cdot \nabla \Phi + gZ \right) \right] (\vec{\xi}_{Rf} \times \vec{N}) dS \\
 & - \rho \iint_{\bar{s}_B} \left[\frac{\partial \Phi}{\partial t} - \vec{U} \cdot \nabla \Phi + \frac{1}{2} \nabla \Phi \cdot \nabla \Phi + gZ \right] (\mathbf{H}_f \vec{N}) dS
 \end{aligned}$$

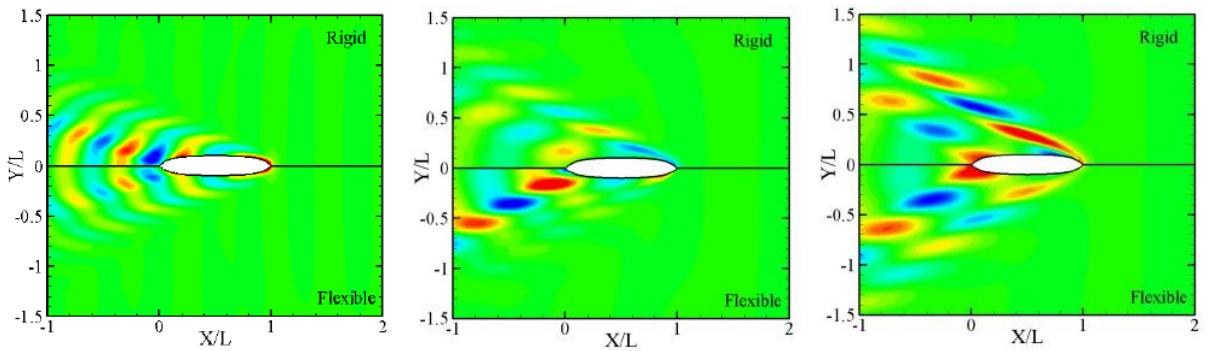
where, $\vec{\xi}_{Tot,1} = \vec{\xi}_T + \vec{\xi}_R \times \vec{X} + \vec{\xi}_{f,av}$, $\xi_{Tot,2} = \mathbf{H}\vec{X} + \vec{\xi}_R \times \vec{\xi}_{f,av}$ (2)

3 RESULTS

As a test model, the blunt modified Wigley model(Kashiwagi, 2003) was used, and the ship speed was fixed at $Fn=0.2$. The flexibility of ship model was manipulated to study the effect of flexible on added resistance; the model is more flexible than that of real ship. Fig.1 shows the structural model and the first two natural modes of the ship model. For this ship, the structural stiffness was determined so that the natural frequencies of 2-node and 3-node vibrations are 0.116 and 0.300 Hz.



Fig. 1 Structural model and the first two vertical bending modes for the modified Wigley model



(a) $\lambda/L=0.5$

(b) $\lambda/L=0.5=1.0$

(c) $\lambda/L=0.5=1.2$

Fig. 2 Instantaneous free surface contours for three different wavelengths

Fig. 2 shows the instantaneous free surface contours for three different wavelengths. From these plots, it can be shown that the hydroelastic effect on free-surface disturbance can be significant. Fig. 3 shows the motion response at two points: the center of bow and the stern of flexible blunt modified Wigley. Compared to the rigid body motion at the bow represented by the red solid-line, the flexible body motion at the bow showed humps and hollows. This trend was induced by the flexible mode (mode 7~). In the wavelength to ship length ratio of 0.5 and 0.9 in Fig. 3, humps were observed. These humps were caused by a match between the natural frequencies of 2- and 3-node vertical vibrations and the encounter frequency of the incident waves.

The added resistance of flexible body is presented in Fig. 4. About the added resistance of flexible body, the results of two numerical methods show good correspondences with each other. Compared with rigid body, added resistance of flexible body increased near the natural frequency of vertical modes and decreased near the similar wave length with ship length. To confirm the phenomenon, the rigidity of ship has increased to two times and four times. For the relatively rigid body, the natural frequency of 2-node vertical mode increased. And the wave length corresponding to the natural frequency of 2-node vertical mode moved as shown Fig. 5. The added resistance increased near the natural frequency of 2-node vertical mode. The added resistance decreased near the similar wave length with ship length and the magnitude of added resistance was in proportion to the rigidity of body.

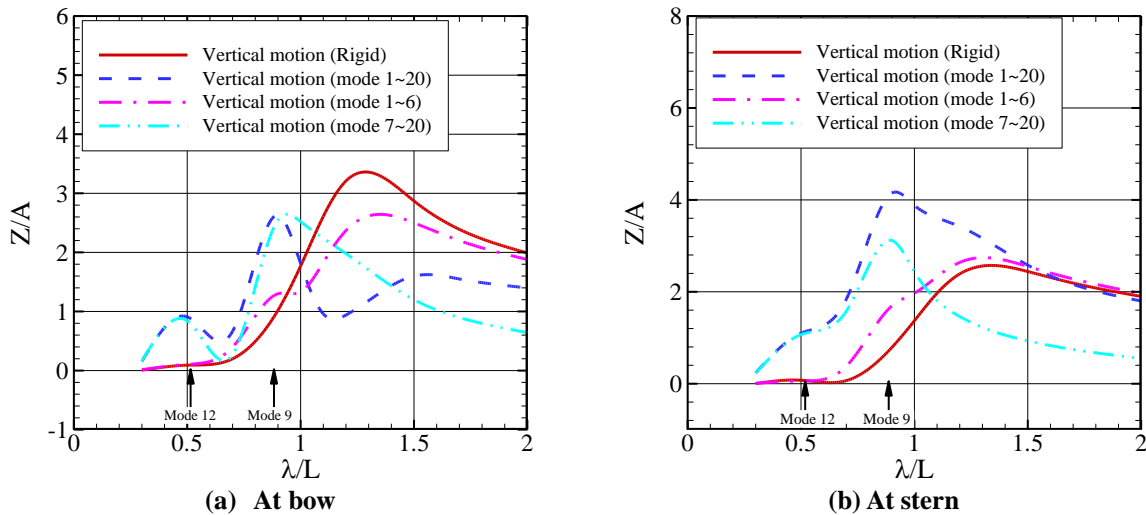


Fig. 3 Vertical motions of flexible body: $F_n=0.2$

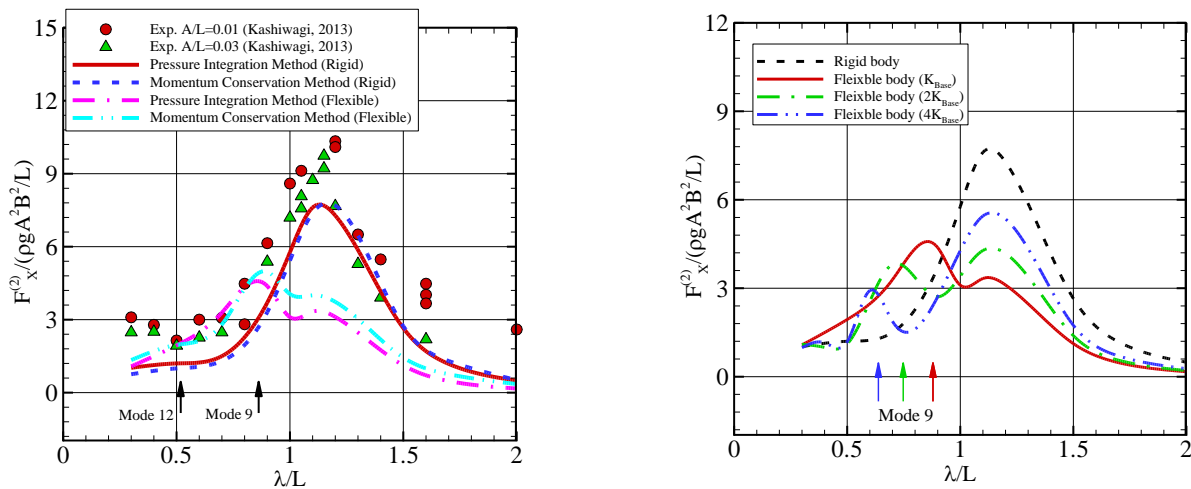


Fig. 4 Comparison of added resistance between rigid and flexible body

Fig. 5 Comparison of added resistance between different flexibility bodies

The dominant contribution of the increase added resistance near the natural frequency of 2-node vertical mode was the increase of relative wave elevation and the change of normal vector due to the deformation of the flexible body. And the decrease in relative wave elevation due to flexible deformation appeared to be the main cause of the decreases added resistance near the wave length with ship length. The shape of the flexible body deformed according to the shape of the incident wave; it is not a resonance response but a quasi-static response. The change in shape decreased the relative motion and disturbed potential.

Fig. 6 shows the sectional distribution of added resistance. The thick bar represents the sectional added resistance of rigid body and the thin bar represents the sectional added resistance of flexible body. Near the natural frequency of 3-node vertical mode ($\lambda/L=0.5$), the added resistance increased in the stern part. On the other hand, near the natural frequency of 2-node vertical mode ($\lambda/L=0.9$), added resistance increased in the middle part of body. In the stern and bow parts, the added resistance of flexible body rather decreased than that of rigid body.

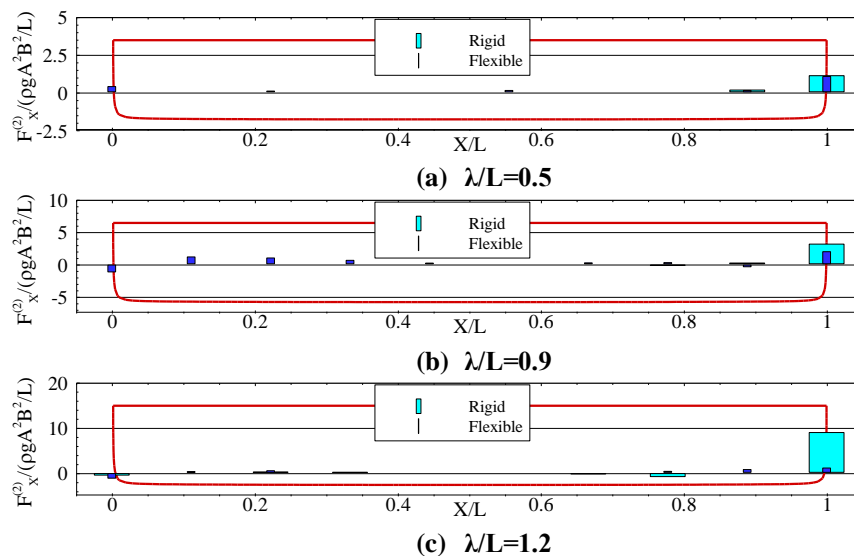


Fig. 6 Sectional added resistance distribution, blunt modified Wigley model, $Fn=0.2$

4 CONCLUSIONS

Based on the present study, the following conclusions can be made:

- For computing the added resistance of a flexible body, the extended pressure integration method was suggested. The results of the pressure integration method showed good agreement with those of the momentum conservation method
- Added resistance of flexible body is dependent in the flexibility of ship structure. In general, Added resistance of flexible body increased near the natural frequency of vertical mode and decreased near the similar wave length the body length.

ACKNOWLEDGEMENTS

This study was supported by the Korean Ministry of Knowledge Economy (MKE), project number 10040030, and the LRF*-Funded Research Center at Seoul National University. Their supports are greatly appreciated.

REFERENCES

- Kashiwagi, M. 2013. Hydrodynamic study on added resistance using unsteady wave analysis. *J. Ship Res.*, 57, pp. 220-240.
- Kim, J.H., Kim, Y., Yuck, R.H. and Lee, D.Y. 2015. Comparison of slamming and whipping loads by fully coupled hydroelastic analysis and experimental measurement. *J. Fluid Struct.*, 52, pp. 145-165.
- Kim, K.H., Seo, M.G. and Kim, Y. 2012. Numerical Analysis on Added Resistance of Ships. *Int. J. Offshore Polar Eng.*, 22, pp. 21-29.
- Park, D.M. Kim, J.H., Kim, Y. 2017. Numerical Study of Mean Drift Force on Stationary Flexible Barge, *Journal of Fluids and Structures* (submitted for publication)